



Oil spill modeling in deep waters: Estimation of pseudo-component properties for cubic equations of state from distillation data

Jonas Gros^{a,*}, Anusha L. Dissanayake^{a,2}, Meghan M. Daniels^a, Christopher H. Barker^b, William Lehr^b, Scott A. Socolofsky^{a,*}

^a Zachry Department of Civil Engineering, Texas A&M University, College Station, TX 77843, USA

^b NOAA Emergency Response Division, Seattle, USA

ARTICLE INFO

Keywords:

Oil spill model
TAMOC
Pseudo-component
Critical properties
GNOME
ADIOS

ABSTRACT

Deep-water oil spills represent a major, localized threat to marine ecosystems. Multi-purpose computer models have been developed to predict the fate of spilled oil. These models include databases of pseudo-components from distillation cut analysis for hundreds of oils, and have been used for guiding response action, damage assessment, and contingency planning for marine oil spills. However, these models are unable to simulate the details of deep-water, high-pressure chemistry. We present a new procedure to calculate the chemical properties necessary for such simulations that we validate with 614 oils from the ADIOS oil library. The calculated properties agree within 20.4% with average values obtained from data for measured compounds, for 90% of the chemical properties. This enables equation-of-state calculations of dead oil density, viscosity, and interfacial tension. This procedure enables development of comprehensive oil spill models to predict the behavior of petroleum fluids in the deep sea.

1. Introduction

Computer models (Reed et al., 1999; Spaulding, 2017) play a critical role for contingency planning, emergency response, and post-spill assessment of marine oil spills (*Oil in the Sea III: Inputs, Fates, and Effects*, 2003). Common operational oil spill models, including OSCAR (Reed et al., 2000), SIMAP/OILMAP (French McCay et al., 2015a; Spaulding et al., 1992), and the General NOAA Operational Modeling Environment (GNOME)/Automated Data Inquiry for Oil Spills (ADIOS) (Lehr et al., 1992, 2000, 2002; Zelenke et al., 2012a, 2012b) have subroutines that simulate the weathering processes that occur when oil is released into the aqueous environment (Spaulding, 2017). Many of these algorithms were developed for surface spills, and the modeled processes include surface spreading, evaporation, water-in-oil emulsification, oil-in-water dispersion, dispersion into the water column, oil-sediment aggregation, response actions, beaching, and, in some models, biodegradation, and ‘marine snow’ formation (Dissanayake et al., 2018a; Passow et al., 2012). These weathering processes alter the bulk properties of the oil, including density, viscosity, pour point, interfacial tension, and adhesion characteristics, and thus, affect its transport. In deep-water oil spills, such as from an accidental oil well blowout or

pipeline leak, real-fluid equations of state (EOS), such as the Peng-Robinson EOS are needed to estimate petroleum fluid properties at the high pressure and low temperature of the deep ocean (Gros et al., 2016). Such cubic EOS require several detailed properties of each component of the oil, and in this paper we develop algorithms to estimate these properties from commonly available distillation-cut data. These algorithms are important to build models of oil that yield adequate predictions in deep-water oil spills.

Unfortunately for oil spill modelers, the oil characteristics data available before a spill occurs is usually limited to characteristics useful to oil industry needs. This typically includes distillation cuts, which provide mass fractions of the oil that boil at a certain temperature or above. Although crude oils are mixtures of thousands of unique hydrocarbons, industry often groups these hydrocarbons for distillation cut reporting into four structural categories, which include saturates, aromatics, resins, and asphaltenes (SARA) (Fan et al., 2002). In general, aromatics tend to be the most aqueously soluble, followed by saturates, which typically have more than an order of magnitude lower solubilities than aromatics with the equivalent carbon number (Schwarzenbach et al., 2003). Resins and asphaltenes are mostly insoluble under the time scales important to the average spill model run.

* Corresponding authors.

E-mail addresses: jonas.gros@alumni.epfl.ch (J. Gros), ssocolofsky@civil.tamu.edu (S.A. Socolofsky).

¹ Present address: GEOMAR Helmholtz Centre for Ocean Research Kiel, Kiel, 24148, Germany.

² Present address: RPS Ocean Science, South Kingstown, RI 02879, USA.

Consequently, an oil is customarily simulated in a response model using a set of 10 to 30 pseudo-components, which are groups of identified or unidentified compounds that share similar properties, with several model pseudo-components covering various aromatics and saturates and two pseudo-components tracking resins and asphaltenes. Each pseudo-component evaporates, aqueously dissolves, and, in some models, biodegrades at rates that are functions of its chemical properties. This type of chemical characterization of oils has been widely used for the modeling of sea-surface oil spills (Spaulding, 2017) where evaporation largely dominates over aqueous dissolution (Gros et al., 2014; Harrison et al., 1975; Radović et al., 2012; Stout and Wang, 2007). However, because each pseudo-component contains many different molecules, it is difficult to determine the pseudo-component properties needed for the type of EOSs that have to be used in deep waters.

In deep waters, an oil spill includes several specific processes: droplet and bubble formation (Bandara and Yapa, 2011; Brandvik et al., 2013; Z. Li et al., 2017; Nissanka and Yapa, 2016; Wang et al., 2018; Zhao et al., 2014, 2017), vertical ascent in a near-field plume (Dissanayake et al., 2018b; Lee and Cheung, 1990; Zheng et al., 2003), formation of a subsurface intrusion (Dissanayake et al., 2018b; Socolofsky et al., 2011), and far-field ascent as individual droplets or bubbles (Clift et al., 1978; Dissanayake et al., 2018b; Fan et al., 1999; Zheng et al., 2003). Dominant oil-spill models usually include a deep-water plume module. However, the equations of state used in these models have limited abilities to predict the non-ideal petroleum chemistry taking place under the high pressures encountered in deep waters (Camilli et al., 2012; Fingas, 2017; Gros et al., 2016, 2017; McNutt et al., 2012; Zick, 2013a, 2013b). This includes both the aqueous solubilities within petroleum mixtures (de Hemptinne et al., 1998; Dhima et al., 1998, 1999; Gros et al., 2016), equilibrium repartitioning of petroleum compounds between petroleum gas and liquid phases (Fingas, 2017; Gros et al., 2016; Zick, 2013a, 2013b), and potential clathrate hydrate formation (Anderson et al., 2012). These processes are highly relevant to the fate of petroleum in deep waters: for example, the light, methane-to-propane hydrocarbons were predicted to have been > 50% partitioned into the petroleum liquid phase when released at ~1500-m depth in the Gulf of Mexico during the 2010 *Deepwater Horizon* oil spill (Gros et al., 2016). In this paper, we focus on deep-water oil spills and on the simulation of the non-ideal deep-water petroleum chemistry for a variety of oils.

Detailed simulation of deep-water petroleum chemistry requires inclusion of a specific thermodynamic model, which is not yet embedded within mainstream oil spill models. We have implemented such a thermodynamic model (Gros et al., 2016) in the Texas A&M Oil spill Calculator (TAMOC) (Dissanayake et al., 2018b; Dissanayake and Socolofsky, 2015; Gros et al., 2017; Socolofsky et al., 2015b). Based on the Peng-Robinson equation of state with volume translation, the modified Henry's law, and other empirical expressions (Gros et al., 2016; King, 1969; Krichevsky and Kasarnovsky, 1935; Lin and Duan, 2005; Peng and Robinson, 1976; Robinson and Peng, 1978; Schwarzenbach et al., 2003), properties of petroleum phases and equilibrium partitioning of components in the gas-oil-water system are predicted (Gros et al., 2016). These simulations require the knowledge of several properties of the modeled pseudo-components that are typically not available in traditional oil spill models, including critical properties (i.e. properties at the critical point), the acentric factor, the Henry's law constant at standard conditions, the partial molar volume at infinite dilution in water, the enthalpy of phase transfer from gas phase to aqueous phase, the Setschenow constant, the molar weight, and the molar volume of each pseudo-component at its normal boiling point.

TAMOC also predicts the dynamic behavior of individual droplets and bubbles of petroleum in deep waters, including aqueous-dissolution kinetics and plume hydrodynamics leading to the formation of a deep-water intrusion due to a density stratification, both under cross-current

and no-current conditions (Dissanayake et al., 2018b; Gros et al., 2017; Socolofsky et al., 2015b). This model was applied to a typical day after the riser was cut during the *Deepwater Horizon* oil spill, and simulations agreed satisfactorily with field observations both in the deep sea and at the sea surface (Gros et al., 2017). TAMOC is relatively similar to other deep-water oil spill models (Johansen, 2003; Zheng et al., 2003) with the additional benefit of a detailed prediction of deep-water petroleum chemistry (Gros et al., 2016, 2017; Socolofsky et al., 2015b), and the inclusion of a model for cases in stratified environments where the cross-current is negligible (Socolofsky et al., 2008). However, TAMOC is focused on the near-field, and for far-field simulations it has to be coupled with another model such as GNOME, which includes horizontally-variable water currents in the water column and on the sea surface, other relevant modules, as well as an oil library. The GNOME model simulates aqueous dissolution of liquid petroleum components, similar to SIMAP/OILMAP. But these models do not enclose an embedded capability to perform flash calculations for simulating gas-liquid equilibrium repartitioning of petroleum compounds. SIMAP/OILMAP has been previously coupled to an external software capable of such calculations through the use of so-called “black oil tables” (Spaulding et al., 2015), however such offline coupling provides limited ability to consider the effect of changing composition. TAMOC has also been previously coupled to the oil spill module in the Modelo Hidrodinámico (P. Li et al., 2017), however no details on the handling of chemistry was provided.

Here we present a method to calculate the required chemical properties for the pseudo-components in TAMOC from the data available in the ADIOS oil library, an open-source database that includes measured data complemented with several estimated properties for > 700 entries. The effort here is important to enable the seamless coupling of TAMOC and GNOME simulations. This new method is transferable to the similar set of pseudo-components used in other oil spill models and therefore allows the coupling of the TAMOC near-field model to a broad range of oil spill models.

2. Methods: model and available data

2.1. Near-field deep-water oil-spill model

To model the deep-water plume hydrodynamics and high-pressure chemistry of petroleum fluids, we selected the TAMOC model that was previously validated to field and laboratory data, including field data from the *Deepwater Horizon* disaster (Dissanayake et al., 2018b; Gros et al., 2016, 2017). TAMOC is an open-source software implemented in Python and Fortran, which is described in more detail in previous literature (Dissanayake et al., 2018b; Dissanayake and Socolofsky, 2015; Gros et al., 2016, 2017; Socolofsky et al., 2015b). The latest version of the model is available at: <https://github.com/socolofs/tamoc> (Socolofsky, 2017), and the version previously used to simulate the *Deepwater Horizon* oil spill is available at: <https://data.gulfresearchinitiative.org> (doi: <https://doi.org/10.7266/N7DF6P8R>). TAMOC includes a three-phase plume model that simulates detailed kinetics of aqueous dissolution, in addition to the prediction of trajectories of bubbles, droplets, and entrained ambient water.

In this work we used only a few modules of TAMOC, principally the thermodynamic model and the modules to estimate properties of bubbles and droplets, as well as the bent plume model. The thermodynamic model is based on the Peng-Robinson equation of state (Peng and Robinson, 1976; Robinson and Peng, 1978), which is a widely-used model to predict gas-liquid equilibrium partitioning of petroleum components and their densities and fugacities. A volume translation method (Lin and Duan, 2005) is applied which ensures accurate predictions of densities for both gas and liquid phases (Gros et al., 2016; Young et al., 2017). Aqueous solubilities are estimated using a modified Henry's law approach (Dhima et al., 1999) including corrections for pressure (King, 1969; Krichevsky and Kasarnovsky, 1935), temperature

(Schwarzenbach et al., 2003), and salinity (Schwarzenbach et al., 2003; Xie et al., 1997), as presented previously (Gros et al., 2016). The thermodynamic model can be applied to any number of components (identified compounds or pseudo-components), from a single-component mixture to mixtures containing hundreds of components (Gros et al., 2016, 2017; Socolofsky, 2017). Thermodynamic-model calculations are based on a set of chemical properties of the pseudo-components: the critical pressure (P_c), the critical volume (V_c), the critical temperature (T_c), the acentric factor (ω), the Henry's law constant at standard conditions ($K_{H,s}$), the partial molar volume at infinite dilution in water (\bar{v}^L), the enthalpy of phase transfer from gas phase to aqueous phase ($\Delta H_{\text{gas} \rightarrow \text{H}_2\text{O}}$), the Setschenow constant (K_{salt}), the molar weight (M), and the molar volume of each component at its normal boiling point (V_b). Thermodynamic-model calculations are also based on the composition of the petroleum fluid (mass fractions of the different components). In this paper, the only modification we have made relative to our previous publication (Dissanayake et al., 2018b) is to update TAMOC to include a new formula for heavy oils for prediction of oil viscosity (Pedersen et al., 2014). Together with the existing algorithms, these methods constitute a comprehensive equation of state for oils given the necessary input parameters.

2.2. Oil pseudo-component library

The pseudo-component simulation of oils follows similar strategies in dominant oil spill models, and here we applied our methods to the ADIOS oil library, developed by the National Oceanographic and Atmospheric Administration (NOAA) of the United States. The oil library was downloaded from: <https://github.com/NOAA-ORR-ERD/OilLibrary> on December 2016. This oil library reports a series of pseudo-components for 736 oils. For each pseudo-component, the mass fraction in the petroleum fluid is listed for several distillation cuts. The ADIOS oil library provides a database of measurements for a few bulk oil properties such as density, viscosity, and (occasionally) interfacial tension with seawater. These properties are reported at one (or a few) temperature(s). Additionally, the oil library includes selected algorithms to estimate values of density, molar weight, boiling point, vapor pressure, and aqueous solubility for these pseudo-components. The data in the ADIOS oil library have been collected from a wide range of sources over the years and provide a very diverse panel of oils to the modeler.

However, the ADIOS oil library was initially not developed for deep-sea oil spills, and some oil characterizations that performed satisfactorily for simulation of sea-surface spills present inconsistent phase information when applied to deep-sea conditions. I.e. that some of the pseudo-components may have the properties of a gas rather than that of a liquid, for some entries of the oil library. To avoid this problem, we eliminated all the oils that were estimated to be > 1% gaseous by mass at 25 °C and 101,325 Pa (1 atm) based on the thermodynamic model implemented in TAMOC (Peng-Robinson equation of state) or that included components having boiling points lower than that of propane. The remaining 614 entries were used in this study.

2.3. Hydrocarbon property database for fitting of new equations

The purpose of this paper is to develop algorithms to estimate the parameters of the Peng-Robinson equation of state from the information in the oil pseudo-component library. To develop new relationships between oil library data and the chemical properties of interest, we use properties of individual petroleum compounds from a database that we previously compiled and have made available (Gros et al., 2016; Gros, 2016). We use these data as is with the single exception that there was a typological error in the latter reference, missing negative signs in $\Delta H_{\text{gas} \rightarrow \text{H}_2\text{O}}$ values. A subset of these data is listed in Table S-5 in the Supporting Information.

3. Methods: algorithm to compute chemical properties

3.1. Chemical-property calculation procedure

In this section, we present a new algorithm that uses properties available within the ADIOS oil library to estimate the parameter values needed in the TAMOC thermodynamic model. This procedure is based on a combination of existing methods and newly-developed property correlations. In this section, we will treat two groups of compounds differently. In the first group, we consider individual compounds with well-known properties. These include several simple chemicals and several pure hydrocarbons with carbon number of six or less (C_1 – C_6 compounds, CO_2 , N_2 , and H_2S). For this group, we will simply use their known chemical properties. In the second group, we consider larger hydrocarbons that will have increasingly complex structures. These are collected into pseudo-component groupings defined by common distillation cut results, and the complete collection of compounds for each pseudo-component is then treated as a single hydrocarbon. It is for the chemical properties of the pseudo-components defined in this second group that we develop this new algorithm.

Our algorithm for estimating the key parameters in TAMOC of these pseudo-component groups from properties available in ADIOS is a two-step process. In the first step, we estimate several fundamental pseudo-component properties directly from the parameters defined in ADIOS, yielding

$$\underbrace{\begin{bmatrix} V_{c,i} \\ P_{c,i} \\ T_{c,i} \\ \omega_i \\ k_{i,j} \\ K_{H^*,i} \end{bmatrix}}_{\text{TAMOC parameters}} = \underbrace{\vec{f}}_{\text{ADIOS parameters}}(VP_i, S_i, M_i, \rho_{\text{ADIOS},i}, T_{b,i}) \quad (1)$$

where i refers to a pseudo-component, $k_{i,j}$ is the binary interaction parameter between pseudo-components i and j in the Peng-Robinson equation of state, VP_i is the vapor pressure of pseudo-component i , S_i is the aqueous solubility of pseudo-component i , $\rho_{\text{ADIOS},i}$ is the density of pseudo-component i , and $T_{b,i}$ is the normal boiling point of pseudo-component i . In a second step, additional parameters are estimated taking advantage of this first set of estimated parameters using relations of the type:

$$\underbrace{\begin{bmatrix} V_{b,i} \\ K_{\text{salt},i} \\ \Delta H_{\text{gas} \rightarrow \text{H}_2\text{O},i} \\ \bar{v}_i^L \end{bmatrix}}_{\text{TAMOC parameters}} = \underbrace{\vec{f}}_{\text{ADIOS parameters and TAMOC parameters}}\left(P_{c,i}, T_{c,i}, V_{c,i}, M_i, \bar{v}_i^L\right) \quad (2)$$

The following sections report the properties for individual compounds, correlations following Eq. (1), and the final set of properties derived by Eq. (2).

3.2. C_1 – C_6 compounds, CO_2 , N_2 , and H_2S

Petroleum fluids in oil reservoirs frequently contain non-negligible mass fractions of these small molecular-weight compounds, with the hydrocarbon compounds (C_1 – C_6) representing the largest contribution (McCain Jr., 1990). These $\leq \text{C}_6$ compounds have well-known properties (Table 1). Consequently, the estimation methods described in the next sections apply only to $> \text{C}_6$ pseudo-components, whereas known values (Table 1) are used for lighter compounds. The ADIOS oil library is focused on liquid petroleum products at atmospheric conditions, which are largely deprived of $\leq \text{C}_5$ compounds. However, these petroleum products could be re-combined for modeling an oil spill with a significant gas-to-oil ratio (GOR), such as a deep-water oil well blowout.

Table 1
Properties of C₁–C₆ compounds, CO₂, N₂, and H₂S.¹

Component	<i>M</i> (g mol ^{−1})	<i>P_c</i> (MPa)	<i>T_c</i> (K)	<i>V_c</i> (cm ³ mol ^{−1})	<i>V_b</i> (cm ³ mol ^{−1})	<i>ω</i> (–)	<i>K_{Hs}</i> (mol m ^{−3} atm ^{−1})	<i>ΔH_{gas→H₂O}</i> (kJ mol ^{−1})	<i>v^L</i> (cm ³ mol ^{−1})	<i>K_{salt}</i> (L mol ^{−1})
C ₁	16.043	4.599	190.56	98.6	37.7	0.011	1.43	−13.1	34.7	0.127
C ₂	30.070	4.872	305.32	145.5	53.5	0.099	1.93	−19.4	50.4	0.162
C ₃	44.097	4.248	369.83	200.0	74.5	0.152	1.50	−22.9	70.7	0.194
<i>i</i> -C ₄	58.123	3.640	407.85	262.7	<u>97.8</u>	0.186	0.87	−24.2	81.3	<u>0.233</u>
<i>n</i> -C ₄	58.123	3.796	425.12	255.0	96.6	0.200	1.20	−25.9	76.6	0.217
<i>i</i> -C ₅	72.150	3.381	460.39	308.3	<u>115.7</u>	0.229	0.73	−25.1	<u>95.4</u>	<u>0.253</u>
<i>n</i> -C ₅	72.150	3.370	469.70	311.0	118.0	0.252	0.81	−28.8	92.3	0.221
C ₆	86.177	3.025	507.60	368.0	<u>139.3</u>	0.300	0.61	−31.6	110.0	0.276
CO ₂	44.010	7.374	304.12	94.1	37.3	0.225	33.94	−19.7	32.0	0.132
N ₂	28.013	3.400	126.20	90.1	34.7	0.0372	0.63	−10.8	33.0	0.183
H ₂ S	34.082	8.963	373.40	98.1	35.2	0.0948	101	−17.9	34.9	0.0462

¹ Values are from literature or estimated (underlined values) as previously described (Gros et al., 2016). The properties of N₂ and H₂S are from the same sources or from other references (Akinfiev and Diamond, 2003; McCain Jr., 1990; Millero, 1986; Wilhelm et al., 1977).

3.3. Critical properties

Critical properties are the main variables driving equations of state for real fluids (Danesh, 1998; McCain Jr., 1990; Pedersen et al., 2014; Riazi, 2005). Several methods to estimate critical properties exist, and their respective predictive abilities have been evaluated in Riazi (2005). We retained two well-established procedures, widely used in the petroleum industry, that performed well in these evaluations. *P_c*, *T_c*, *V_c* are estimated from the Twu correlation (Twu, 1984) and *ω* from the Kesler–Lee correlation (Chen et al., 1993; Lee and Kesler, 1975), which depend on the boiling point and the density of each pseudo-component, as provided by the ADIOS oil library.

These estimates may lead to poor predictions of the densities of petroleum liquids when used as such, and equation of state tuning is a procedure frequently applied in petroleum modeling to improve the predictive ability of equation-of-state models (Zick, 2013a). Tuning is a delicate, empirical procedure that carefully modifies, or “tunes”, one or several critical properties of components in order to match available laboratory data (Zick, 2013a). Here, we tune the values of the critical volume of the pseudo-components, to better match the densities of the pseudo-components predicted with the thermodynamic model to the densities derived from the ADIOS oil library. Our choice of the tuning parameter, *V_c*, was guided by the fact that this property does not affect petroleum gas-liquid equilibrium calculations.

For this specific calculation, we re-defined the densities of the pseudo-components differently than in the ADIOS oil library. Since the volume change on mixing of liquid hydrocarbons is almost zero (usually < 0.1% (ASTM, 1968)), we assumed that:

$$\rho_{oil} \cong \frac{\sum \text{masses}}{\sum \text{volumes}} = \frac{1}{\sum \left(\frac{m_i}{\rho_i} \right)} \quad (3)$$

where ρ_{oil} is the density of an oil as reported in the ADIOS oil library, m_i is the mass fraction of the component *i* in the oil, and ρ_i is the density of that component.

V_{c,i} values are tuned so that the thermodynamic model predicts densities of pseudo-components, $\rho_{TAMOC,i}$ close to ρ_i . ρ_i differs slightly from the pseudo-component densities in the ADIOS oil library, $\rho_{ADIOS,i}$ which are based on the assumption $\rho_{oil} = \sum (m_i \cdot \rho_{ADIOS,i})$ in lieu of Eq. (3). For each pseudo-component *i*, tuning is conducted using a bracketing root-finding method to find the *V_{c,i}* such that $(\rho_i - \rho_{TAMOC,i})$ approaches zero. The procedure is repeated iteratively until the residual is < 10^{−4} cm³ mol^{−1}, meaning that *V_c* is converged. Because ρ_i is always available from the ADIOS database, this tuning can be done for any implementation of our algorithm. Note also that this turning is applied to the calculated densities of each pseudo-component, and not to the density of the whole oil mixture.

3.4. Binary interaction parameters

Cubic equations of state like that of Peng and Robinson (Peng and Robinson, 1976; Robinson and Peng, 1978) include binary interaction parameters that ensure accurate predictions (Pedersen et al., 1988, 2014; Riazi, 2005). There is one binary interaction parameter to characterize each pair of components, and we calculate them based on the method of Pedersen (Pedersen et al., 1988) for hydrocarbon-hydrocarbon interactions:

$$\begin{cases} k_{i,j} = k_{j,i} = 0.00145 \cdot \max \left(\frac{M_j}{M_i}, \frac{M_i}{M_j} \right) & \text{if } i \neq j \\ k_{i,j} = 0 & \text{if } i = j \end{cases} \quad (4)$$

where *M_i* and *M_j* are the molar weights of components *i* and *j*, respectively, and *k_{i,j}* is the binary interaction parameter between components *i* and *j*. Binary interaction parameters between non-hydrocarbon components (CO₂, N₂, and H₂S) and other components were taken from previous literature (Pedersen et al., 2014); their values are reported in Table 2.

3.5. Properties related to aqueous solubility

Because the solubilities of > C₆ saturates, asphaltenes and resins are negligible compared to that of aromatics (Oil in the Sea III: Inputs, Fates, and Effects, 2003), GNOME considers that only the aromatic pseudo-components are aqueously soluble. GNOME estimates the solubility in pure water, *S_{w,i}*, and the vapor pressure, *VP_i*, for each aromatic component *i*. *K_{Hs,i}*, the corresponding Henry's law constant at standard conditions (*), is calculated from:

Table 2
Values of the binary interaction parameters between hydrocarbon-containing pseudo-components and CO₂, N₂, and H₂S (Pedersen et al., 2014).

Component	CO ₂	N ₂	H ₂ S
C ₁	0.1200	0.0311	0.0800
C ₂	0.1200	0.0515	0.0833
C ₃	0.1200	0.0852	0.0878
<i>i</i> -C ₄	0.1200	0.1033	0.0474
<i>n</i> -C ₄	0.1200	0.0800	0.0600
<i>i</i> -C ₅	0.1200	0.0922	0.0600
<i>n</i> -C ₅	0.1200	0.1000	0.0630
C ₆	0.1200	0.0800	0.0500
≥C ₇	0.0100	0.0800	0.0000
CO ₂	0	0.0170	0.0974
N ₂	0.0170	0	0.1767
H ₂ S	0.0974	0.1767	0

$$K_{H^*,i} = \frac{S_{w,i}(T^*, P^*, S^*)}{VP_i(T^*, P^*, S^*)} \quad (5)$$

where T^* , P^* , and S^* are temperature, pressure, and salinity at a standard state of 25 °C, 1 atm, and 0 g kg⁻¹ of salinity. For use in Eq. (5), aqueous solubilities in pure water are calculated from (SI Section S-1):

$$S_{w,i} = 46.4 \cdot 10^{-36.7 \cdot \frac{M_i}{\rho_{ADIOS,i}}} \quad (6)$$

where M_i is in g mol⁻¹, $\rho_{ADIOS,i}$ is in kg m⁻³, and $S_{w,i}$ is in mol L⁻¹. Vapor pressure at standard conditions is taken from the ADIOS oil library.

GNOME assumes that only vapor pressure depends on temperature, and not aqueous solubility. This is a good approximation for saturates and small aromatics, but can lead to overestimates of the Henry's law constant by 100% or more for heavy polycyclic aromatic hydrocarbons (PAHs) (Gros et al., 2014; Schwarzenbach et al., 2003). Consequently, we calculate the $\Delta H_{gas \rightarrow H_2O}$ values for aromatic pseudo-components, used to correct aqueous solubility for temperature (Gros et al., 2016), with a new correlation ($r^2 = 0.91$) fitted to data for 57 aromatic compounds from our hydrocarbon property database:

$$\Delta H_{gas \rightarrow H_2O,i} = -R \cdot (2.637 \cdot T_{c,i} + 22.48 \cdot 10^6 \cdot \bar{v}_i^L + 314.6) \quad (7)$$

where R is the gas constant in units of J mol⁻¹ K⁻¹, $\Delta H_{gas \rightarrow H_2O,i}$ is in J mol⁻¹, $T_{c,i}$ is in K, and \bar{v}_i^L is in m³ mol⁻¹. The root-mean-squared-error (RMSE) is 2970 J mol⁻¹ (relative error of 6%) (Fig. 1b).

We also correct for the effect of salinity on aqueous solubility for marine oil spills. The Setschenow constant, used for this correction, is calculated from (Gros et al., 2016):

$$K_{salt,i} = -1.35 \cdot M_i + 2800 \cdot \bar{v}_i^L + 0.0836 \quad (8)$$

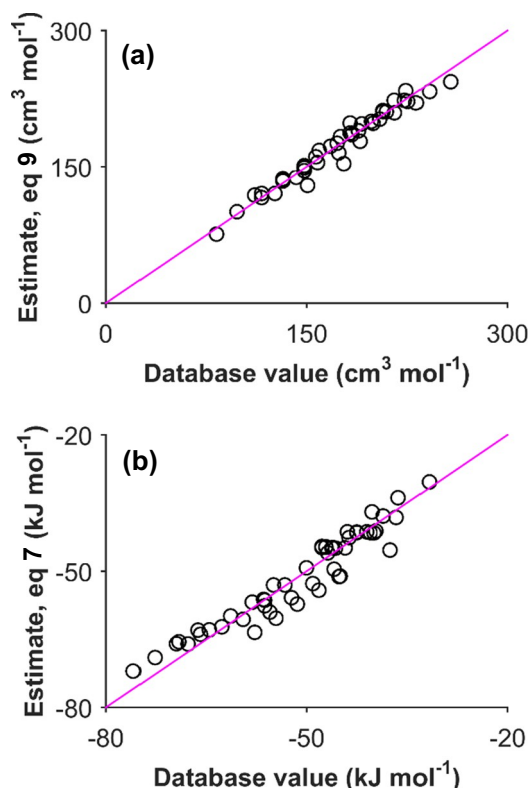


Fig. 1. Validation of (a) Eq. (9) and (b) Eq. (7) with data from 57 aromatic compounds from the hydrocarbon property database (black circles). The identity lines are displayed in pink (having a slope of 1 and an intercept of 0). (For interpretation of the references to colour in this figure legend, the reader is referred to the web version of this article.)

where $K_{salt,i}$ is in L mol⁻¹, M_i is in kg mol⁻¹, and \bar{v}_i^L is in m³ mol⁻¹.

Finally, for a deep ocean spill, we must correct the solubility for the effect of pressure. The method of Lyckman et al. (Lyckman et al., 1965; Shakir and de Hemptinne, 2007) to estimate \bar{v}_i^L applies only to gases (Gros et al., 2016; Lyckman et al., 1965). Consequently, we calculate \bar{v}_i^L values for aromatic pseudo-components with a new correlation ($r^2 = 0.97$) fitted to data for the same 57 aromatic compounds from the hydrocarbon property database as used for Eq. (7), yielding:

$$\bar{v}_i^L = (-2.203 \cdot 10^{-5} \cdot P_{c,i} + 518.6 \cdot M_i + 143.4) \cdot 10^{-6} \quad (9)$$

where $P_{c,i}$ is in Pa, M_i is in kg mol⁻¹, and \bar{v}_i^L is in m³ mol⁻¹. The RMSE is 6.9 cm³ mol⁻¹ (4.1%) (Fig. 1a).

The kinetics of aqueous dissolution also depend on the molecular diffusivity of each pseudo-component in seawater. In order to calculate diffusion coefficients in water based on the Hayduk-Laudie formula (Hayduk and Laudie, 1974), V_b is calculated from the Tyn and Calus formula (Poling et al., 2001):

$$V_{b,i} = 0.285 \cdot (V_{c,i} \cdot 10^6)^{1.048} \cdot 10^{-6} \quad (10)$$

where both $V_{b,i}$ and the critical volume, $V_{c,i}$, are expressed in m³ mol⁻¹. With each of these parameters (Eqs. (1) and (2)) defined, the TAMOC equations of state can be used to simulate oils in the ADIOS oil library.

4. Results

4.1. Validation with bulk properties of oils from the ADIOS oil library

As a first validation test, we compared predictions of the oil bulk properties (density, viscosity, and interfacial tension between oil and seawater) for 614 oils of the ADIOS oil library with predictions from the thermodynamic model using pseudo-component chemical properties calculated with our procedure. The densities estimated in TAMOC are predicted to within 8.7 kg m⁻³ for 95% of the oils evaluated, when the tuning of V_c is conducted following our method presented above (Fig. 2b). For most oils, this level of precision is sufficient for ensuring minimal effect on model predictions. However, three heavy oils would be predicted to slowly sink within a seawater having a density of

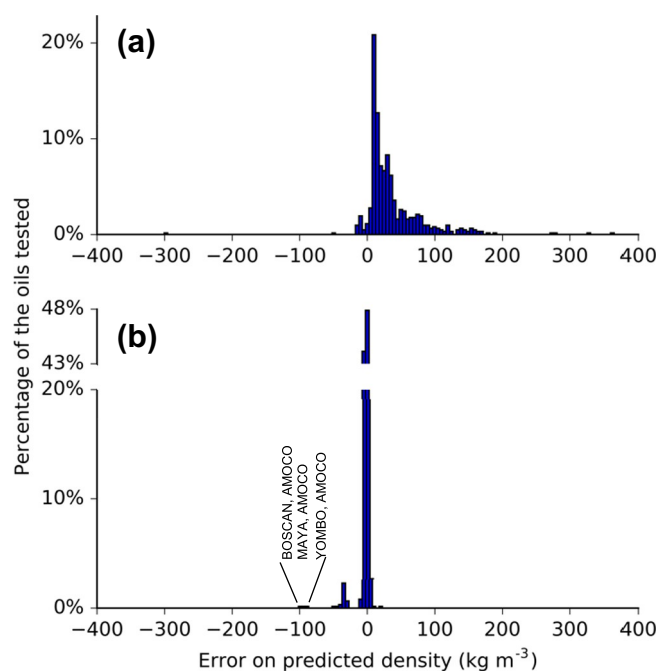


Fig. 2. Difference between TAMOC thermodynamic-model oil densities and oil densities from the ADIOS oil library (a) without tuning of V_c and (b) with tuning of V_c .

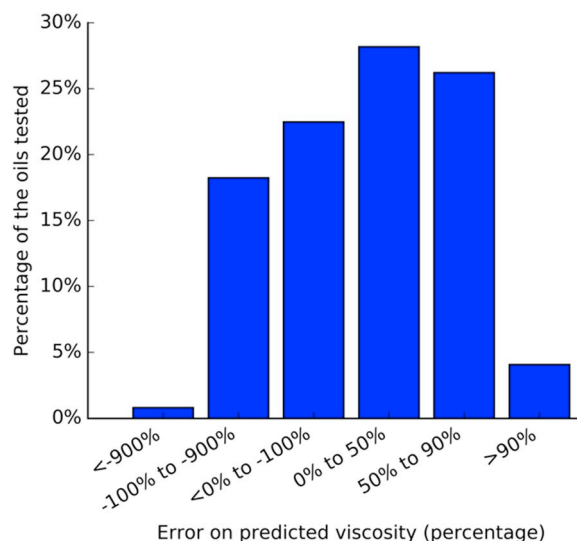


Fig. 3. Relative error between TAMOC thermodynamic-model dynamic viscosities and measured dynamic viscosities from the ADIOS oil library. Here $relative\ error = \frac{data - estimate}{data}$. An overestimate by a factor of two (estimate = 2 · data) is a -100% relative error, whereas an underestimate by a factor of two is a 50% relative error. The set of bars represent over- and underestimates by factors of 1–2, 2–10, and > 10.

1025 kg m⁻³, in disagreement with their densities reported in the ADIOS oil library. These three heavy oils are two Venezuelan oils—‘BOSCAN, AMOCO’ and ‘TIA JUANA PESADO’ (Carnahan et al., 1999; Pilcher and Winterbottom, 1988)—, and a Congolese oil—‘YOMBO, AMOCO’. Prediction of oil sinking is a complex task. The density of an oil may differ from its database density value due to normal evolution of oil composition over the life time of an oil field, and determination of the point in time when an oil becomes denser than seawater is dependent on the assumptions made in the simulation of evaporation, such as

oil slick thickness.

Dynamic viscosity is estimated within a factor of 2 for 51% of the oils evaluated and within a factor of 10 for 95% of the oils evaluated (Fig. 3). Similarly large uncertainties for dynamic viscosities of petroleum liquids are to be expected due to the limited predictive abilities of existing methods (Riazi, 2005). However, dynamic viscosity is not a sensitive parameter in TAMOC simulations. Derived properties such as slip velocities of droplets have ≤35% uncertainty arising from the uncertainties on dynamic viscosity for 98% of the cases. This is regarded as reasonable due to the large uncertainties associated with estimates of slip velocities (Clift et al., 1978; Fan et al., 1999). Additionally, the dynamic viscosity of an oil may affect the prediction of initial size distributions of droplets for very viscous oils or oils for which their interfacial tension with seawater has been profoundly depleted by addition of chemical dispersant (Z. Li et al., 2017; Zhao et al., 2014).

The ADIOS oil library includes few entries of interfacial tension between oil and seawater. Predictions agree with available data within a factor of 10, based on data for 12 oils (Table S-2). Interfacial tension is not a controlling parameter for deep-sea oil-well blowouts except for initial size distributions of droplets (Johansen et al., 2013; Z. Li et al., 2017; Zhao et al., 2014). We advise that a measured value of the interfacial tension is used to scale the predictions of TAMOC whenever available, especially in order to predict initial size distributions. Oil-water interfacial tension is also a key parameter controlling recovery of oil from reservoirs, stability of oil-water emulsions, and transport of organic contaminants through soils (Andersson et al., 2014), and several estimation methods have been presented (Andersson et al., 2014; Danesh, 1998; Firoozabadi and Ramey, 1988; Kalantari Meybodi et al., 2016; Kim and Burgess, 2001; Najafi-Marghmaleki et al., 2016; Papavasileiou et al., 2017). However, very few methods are applicable to poorly-defined liquid hydrocarbon mixtures such as oils at conditions of temperature and pressure in the deep ocean. Consequently, prediction of interfacial tension with seawater remains a difficult task (Danesh, 1998), as oils having similar properties can exhibit different interfacial tensions with seawater (Government of Canada, 2017), which prevents the easy development of accurate estimation methods.

Table 3

Difference between estimated properties (Prop) of pseudo-components from the ADIOS oil library for Louisiana Sweet crude oil calculated using our procedure with respect to using the arithmetic average of the properties of individual compounds included in the pseudo-components. Negative values denote larger values predicted by the second method, and they are expressed as a percentage $\left(\frac{Prop_{our\ procedure} - Prop_{included\ compounds}}{Prop_{our\ procedure}} \right)$.

Component	M	P _c	T _c	V _c	V _b	ω	K _{Hs}	ΔH _{gas→H₂O}	\bar{v}^L	K _{salt}
Saturates1	13.9%	-6.0%	-7.7%	-5.2%	-5.6%	16.0%	- ^a	- ^a	- ^a	- ^a
Aromatics1	11.0%	-17.6%	-7.8%	1.1%	-0.2%	-9.1%	-172%	-3.8%	6.5%	15.1%
Saturates2	0.4%	-14.1%	-2.0%	7.4%	7.7%	24.5%	- ^a	- ^a	- ^a	- ^a
Aromatics2	-0.8%	-17.4%	-1.9%	7.0%	7.9%	-1.6%	-147%	1.2%	14.7%	13.9%
Saturates3	-1.4%	-11.9%	-1.1%	6.7%	7.0%	20.4%	- ^a	- ^a	- ^a	- ^a
Aromatics3	4.0%	-4.0%	-1.5%	-4.2%	-4.4%	-9.6%	-150%	-1.2%	0.9%	0.5%
Saturates4	1.9%	-1.6%	-1.6%	-5.3%	-5.6%	7.6%	- ^a	- ^a	- ^a	- ^a
Aromatics4	-11.9%	-15.5%	1.1%	20.5%	21.4%	31.6%	-232%	6.4%	8.5%	3.5%
Saturates5	-0.1%	-1.6%	-0.9%	-8.4%	-8.9%	8.5%	- ^a	- ^a	- ^a	- ^a
Aromatics5	-20.7%	-43.1%	-3.8%	25.6%	26.7%	22.6%	-7110%	10.8%	20.7%	15.6%
Saturates6	3.1%	-0.7%	-1.1%	-14.3%	-15.1%	1.2%	- ^a	- ^a	- ^a	- ^a
Aromatics6	-23.3%	-40.8%	-3.4%	25.6%	26.6%	19.6%	-2.5·10 ⁴ %	17.5%	21.2%	16.3%
Saturates7	0.4%	4.1%	-0.1%	-26.3%	-27.8%	-0.7%	- ^a	- ^a	- ^a	- ^a
Aromatics7	-29.1%	-33.4%	-3.3%	31.6%	32.8%	19.7%	-1.4·10 ⁵ %	17.4%	23.6%	13.8%
Saturates8	-0.9%	2.7%	1.1%	-32.9%	-34.7%	-4.3%	- ^a	- ^a	- ^a	- ^a
Aromatics8	-33.5%	-31.7%	-6.0%	33.8%	35.1%	19.7%	-1.8·10 ⁶ %	16.1%	25.5%	11.9%
Saturates9	-6.2%	-9.1%	2.6%	-32.3%	-34.1%	-2.3%	- ^a	- ^a	- ^a	- ^a
Aromatics9	-38.7%	-39.0%	-5.8%	38.3%	39.7%	25.7%	-2.6·10 ⁷ %	18.0%	30.7%	15.8%
Saturates10	-	-	-	-	-	-	- ^a	- ^a	- ^a	- ^a
Aromatics10	-44.6%	-45.4%	-3.9%	44.7%	46.3%	32.2%	-1.2·10 ⁸ %	20.2%	34.8%	21.6%
Average	-9.3%	-17.2%	-2.5%	6.0%	6.0%	11.7%	-1.5·10 ⁷ %	10.3%	18.7%	12.8%
AAD ^b	12.9%	17.9%	3.0%	19.5%	20.4%	14.6%	1.5·10 ⁷ %	11.3%	18.7%	12.8%
Min	-44.6%	-45.4%	-7.8%	-32.9%	-34.7%	-9.6%	-1.2·10 ⁸ %	-3.8%	0.9%	0.5%
Max	13.9%	4.1%	2.6%	44.7%	46.3%	32.2%	-147%	20.2%	34.8%	21.6%

^a Insoluble components.

^b Average absolute deviation.

Table 4
Example properties of a reservoir fluid including C₁–C₅ compounds, derived based on Louisiana Sweet crude oil, assuming a gas-to-oil ratio (GOR) of 2000 standard cubic feet per barrel. Predictions are based on a single-stage gas-liquid equilibrium calculation for the reservoir fluid.

Property	20 MPa and 423.15 K (hot fluids exiting the sea floor, ~2000-m water depth)	20 MPa and 278.15 K (fluids cooled to temperature of ambient water, ~2000-m water depth)	0.101325 MPa and 288.15 (sea surface)
Gas density (kg m ⁻³)	132 ^a	212 ^a	0.85 ^a
Petroleum liquid density (kg m ⁻³)	678	706	854
Volume fraction occupied by gas	58%	26%	99.7%
Methane in gas phase	73%	42%	99.8%
Methane in liquid phase	27%	58%	0.2%

^a Differs from the density of pure methane (91, 175, and 0.68 kg m⁻³, respectively) due to the presence of larger molecules in the gas phase.

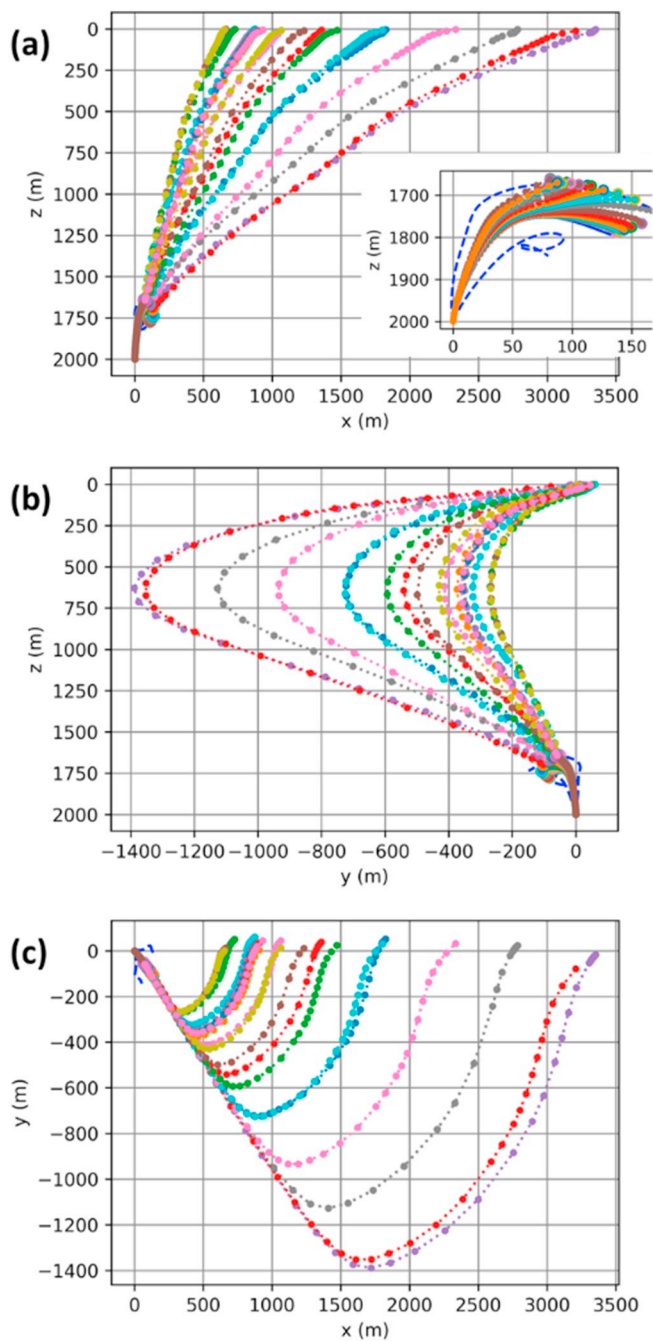


Fig. 4. Oil droplet and gas bubble trajectories predicted within the 10-km diameter cylinder centered at the emission source tracked with TAMOC. This includes the predicted plume formed of bubbles, droplets, and entrained water (depicted with the dashed blue line), overlaid with predicted trajectories of bubbles and droplets of different diameters (other colored lines). Panels a–c depict three different projections. The inset on panel a provides a zoom on the plume region. (For interpretation of the references to colour in this figure legend, the reader is referred to the web version of this article.)

4.2. Comparison of component properties with properties of individual compounds

As a second validation test, we compared the calculated properties of the components of Louisiana Sweet crude oil derived as described above (Table S-3) with the properties obtained by taking the arithmetic average of properties of individual compounds within the corresponding boiling point range of each component (Table S-6). Excluding the Henry's law constant (discussed below), the average absolute

deviation for all properties is $\leq 20.4\%$ (Table 3). The arithmetic average of values for a series of individual compounds is not regarded as superior to our procedure presented above. However, closely aligned results between the two procedures indicate a satisfactory behavior of the new method.

Systematic differences between properties of pseudo-components estimated in these two ways exist for saturate versus aromatic pseudo-components. Saturate pseudo-components usually exhibit better correspondence between the two estimates (Table 3). This may arise from different levels of uncertainties in the estimated base properties (ρ_{ADIOS} , M) of saturates and aromatics within the ADIOS oil library. However, this could also reflect a bias in the individual compounds having available data. The heaviest pseudo-components include a mixture of hundreds or thousands of poorly identified compounds, however, only PAHs and normal alkanes were used for pseudo-components having normal boiling points $> 584.3\text{ K}$ (Table S-5). For example, the contribution of monoaromatics to the properties of the heaviest aromatic pseudo-components is not considered (by lack of data) when preparing Table S-6. The case of M is discussed below in more details in the context of the results obtained for the Henry's law constant.

Contrary to other properties, Henry's law constants are up to 6 orders of magnitude lower for the heaviest aromatic pseudo-components when estimated from GNOME pseudo-components rather than the average values of individual compounds (Table 3). This implies that our estimated parameters would underestimate aqueous dissolution for these components compared to real compounds in our database. This discrepancy between the two sets of estimates arises because, through the estimate of M (Riazi, 2005), GNOME assumes that the solubility of aromatic components can be based on that of n -alkylbenzenes. However, the individual compounds used to compute average values are all PAHs for the heaviest aromatic components (having $T_b > 535$). If the M values from the included compounds (Table S-6) are used in Eq. (6), predicted values of K_{H_s} agree within 84% with the average of the K_{H_s} of the individual compounds, for all pseudo-components studied except the little-soluble aromatics10 (-382% deviation). Similar discrepancies of several orders of magnitude for K_{H_s} between mono-aromatic and poly-aromatic hydrocarbons of large chain length are deduced from the group-contribution estimation method of Hine and Mookerjee (Gros, 2016; Hine and Mookerjee, 1975). Therefore, the estimates used in GNOME are more accurate for alkylated mono-aromatics than poly-aromatic compounds. Quantification of their respective mass fractions using two-dimensional gas chromatography techniques have indicated that mono-aromatic hydrocarbons and PAHs both contribute significantly to the mass of high-boiling aromatic compounds for Macondo oil (Gros, 2016). Consequently, no accurate prediction of the aqueous dissolution of heavy, sparingly-soluble, aromatic pseudo-components can be issued for oils in the ADIOS oil library as compounds having estimated aqueous solubilities spanning several orders of magnitude are lumped together within a single pseudo-component. Accurate predictions of aqueous dissolution require splitting of the GNOME aromatic pseudo-components into mono-aromatics, bi-aromatics, tri-aromatics, etc. (SI Section S-5). However, this has a limited impact on model predictions because these pseudo-components wouldn't dissolve noticeably under normal oil spill conditions (Oil in the Sea III: Inputs, Fates, and Effects, 2003), even in deep waters (Reddy et al., 2012; Ryerson et al., 2012) over timescales of interest to oil spill response and water column damage assessment. Consequently, these sets of pseudo-components will perform satisfactorily for modeling targeted at guiding response action.

4.3. Implications for the modeling of deep-water oil spills

Traditional sets of pseudo-components used in oil spill models are readily available for hundreds of crude oils through oil libraries such as the ADIOS oil library. These oil libraries allow for fast predictions in the case of accidental spills. Here we extend the use of these pseudo-

components for deep-water oil spills. Consideration of the effect of high pressure on the behavior of petroleum components becomes crucial when light C_1 – C_5 components are present, which is likely for a release from an accidental oil well blowout.

As an example, we simulated a fictitious but realistic release scenario not tailored to a specific location. The simulated release consists of Louisiana Sweet crude oil with a gas-to-oil ratio (GOR) of 2000 standard cubic feet per barrel of oil, for a scenario similar to case 1 of a previous article (Socolofsky et al., 2015a). This reservoir fluid is made of Louisiana Sweet crude oil (from ADIOS oil library) and natural gas (composition of gas from (Socolofsky et al., 2015a)). Droplets and bubbles were tracked with TAMOC within a 10-km radius cylinder centered at the emission source. Droplets or bubbles exiting this cylinder either laterally or upon reaching the sea surface were handed to GNOME to track their fate in the water column and/or at the sea surface, here using a time step of 30 min in GNOME. Three-dimensional water currents in the TAMOC and GNOME simulations are based on HYCOM model predictions. The initial size of droplets and bubbles were assumed to follow Rosin-Rammler distributions (Johansen et al., 2013), assuming a 3.8 mm (Socolofsky et al., 2015a) and 5 mm (Wang et al., 2018) volume median diameter, respectively. The diameter of the release orifice (emission source) was assumed to be 30 cm.

TAMOC simulations predict that the released reservoir fluid would have $> 58\%$ of its light, C_1 – C_5 components partitioned to the petroleum liquid phase at $\sim 2000\text{-m}$ depth, contrasting with the situation at the sea surface (Table 4 and SI Section S-6). These predictions are based on an equilibrium, single-stage flash calculation (Gros et al., 2016) based on component chemical properties (Tables 1 and S-3). This indicates that liquid-oil droplets have initial densities lower than that of sea-surface dead oil, leading to a 96% initial increase of droplet buoyancy. TAMOC predicts the evolution of these properties during ascent of bubbles and droplets. For example, the density of liquid oil increases upon aqueous dissolution of the C_1 – C_5 components, which are rapidly lost from ascending droplets (Gros et al., 2017), and the densities of droplets rapidly approach the density of liquid oil at sea surface conditions (Socolofsky et al., 2015b).

Fig. 4 depicts the 10-km radius zone simulated with TAMOC upon release from a broken well. Upon exit from the plume, the bubbles and droplets were assumed to rise independently in the water column. After exit from the 10-km radius near-field cylindrical domain defined for TAMOC, droplets and bubbles are further tracked with GNOME indicating likely areas with elevated presence of oil (Fig. 5). These methods therefore enable fast predictions based on components from the ADIOS oil library, making accurate deep-sea simulations available within the short time constraints of emergency response action.

5. Conclusion

Albeit that major deep-sea oil releases represent a significant threat to sensitive environments (French McCay et al., 2015b; White et al., 2012); state-of-the-art oil spill models so far have had limited abilities to simulate deep-water petroleum chemistry. This particularly affects simulation of accidental releases that are likely to include light, C_1 – C_5 compounds, which cannot be considered purely as a separate entity compared to $> C_6$ components at deep-water conditions of pressure and temperature (Table 4). Considering this specific chemistry in oil spill models enables to investigate phase changes happening before release into the sea (e.g. within a broken blowout preventer), as well as to perform a more consistent treatment of oil and gas behavior, leading to more accurate prediction of the repartition of petroleum compounds within the water column. Here we presented a strategy to imbed the TAMOC model, which simulates these deep-water chemistry, within the GNOME oil spill model. The methods leading to this new, open-source coupled modeling tool described here are easily expandable to slightly different sets of pseudo-components used by other major oil spill models such as SIMAP/OILMAP and OSCAR because the overall

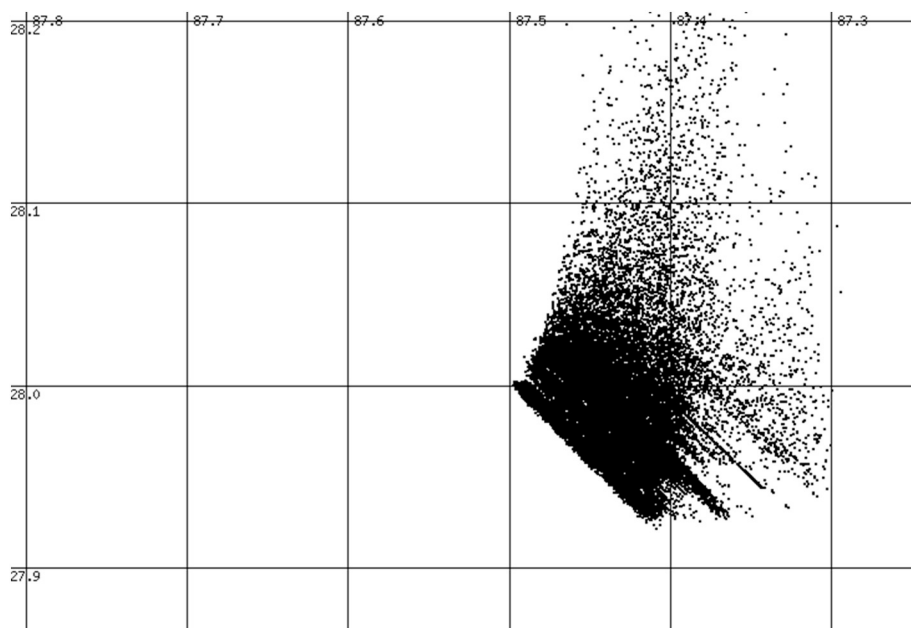


Fig. 5. Two-dimensional projection of Lagrangian elements representing oil within a GNOME simulation of a release of Louisiana Sweet crude oil with gas (GOR = 2000), 24 h after the start of a continuous release at 2000-m depth. (Arbitrary) latitudes and longitudes are displayed for scale, however the scenario wasn't parameterized for any specific, existing location.

strategy for defining pseudo-components is basically the same across models. Therefore, the proposed selected set of pre-existing and new estimation methods for pseudo-component properties open new perspectives to the whole field of oil spill modeling.

Abbreviations

C_1	methane
C_2	ethane
C_3	propane
$i-C_4$	isobutane
$n-C_4$	normal butane
$i-C_5$	isopentane
$n-C_5$	normal pentane
C_6	normal hexane
$k_{i,j}$	binary interaction parameter between components i and j
K_{H_s}	Henry's law constant at standard conditions (25 °C, 101325 Pa)
K_H	Henry's law constant at non-standard conditions
K_{salt}	Setschenow constant
m	mass fraction
M	molar weight
P_c	critical pressure
S_w	solubility in pure water
T_b	normal boiling point (temperature of ebullition at 101325 Pa)
T_c	critical temperature
\bar{v}^L	partial molar volume at infinite dilution in water
V_b	molar volume at the normal boiling point of the component
V_c	critical volume
VP	vapor pressure
$\Delta H_{gas \rightarrow H_2O}$	enthalpy of phase transfer from gas phase to aqueous phase
ρ_{oil}	density of an oil
$\rho_{ADIOS,i}$	density of pseudo-component i according to the ADIOS oil library
ρ_i	density of pseudo-component i according to Eq. (3)
$\rho_{TAMOC,i}$	density of pseudo-component i according to the thermodynamic model
ω	acentric factor

Acknowledgements

We thank Louis Thibodeaux (Louisiana State University) and Deedar Nabi (National University of Sciences and Technology, Pakistan) for discussions about property estimates, and we are grateful to James Makela and Jay A. Hennen (NOAA) for support with GNOME installation and help with the coding of the coupled codes. This work was supported by the U.S. Department of Homeland Security through the Arctic Domain Awareness Center (ADAC) [grant award number 2014-ST-061-ML0002]. The views and conclusions contained in this document are those of the authors and should not be interpreted as necessarily representing the official policies, either expressed or implied, of the U.S. Department of Homeland security.

Declarations of interest

None.

Appendix A. Supplementary data

Supplementary data to this article can be found online at <https://doi.org/10.1016/j.marpolbul.2018.10.047>.

References

- Akinfiev, N.N., Diamond, L.W., 2003. Thermodynamic description of aqueous nonelectrolytes at infinite dilution over a wide range of state parameters. *Geochim. Cosmochim. Acta* 67, 613–629. [https://doi.org/10.1016/S0016-7037\(02\)01141-9](https://doi.org/10.1016/S0016-7037(02)01141-9).
- Anderson, K., Bhatnagar, G., Crosby, D., Hatton, G., Manfield, P., Kuzmicki, A., Fenwick, N., Pontaza, J., Wicks, M., Socolofsky, S., Brady, C., Svedeman, S., Sum, A.K., Koh, C., Levine, J., Warzinski, R.P., Shaffer, F., 2012. Hydrates in the ocean beneath, around, and above production equipment. *Energy Fuel* 26, 4167–4176. <https://doi.org/10.1021/ef300261z>.
- Andersson, M.P., Bennetzen, M.V., Klamt, A., Stipp, S.L.S., 2014. First-principles prediction of liquid/liquid interfacial tension. *J. Chem. Theory Comput.* 10, 3401–3408. <https://doi.org/10.1021/ct500266z>.
- ASTM, 1968. Standard Method of Test for Aromatic Hydrocarbons in Olefin-Free Gasolines by Silica Gel Adsorption. *Man. Hydrocarb. Anal.* Second ed. <https://doi.org/10.1520/STP31924S>.
- Bandara, U.C., Yapa, P.D., 2011. Bubble sizes, breakup, and coalescence in deepwater gas/oil plumes. *J. Hydraul. Eng.* 137, 729–738. [https://doi.org/10.1061/\(ASCE\)HY.1943-7900.0000380](https://doi.org/10.1061/(ASCE)HY.1943-7900.0000380).
- Brandvik, P.J., Johansen, Ø., Leirvik, F., Farooq, U., Daling, P.S., 2013. Droplet breakup in subsurface oil releases – part 1: experimental study of droplet breakup and effectiveness of dispersant injection. *Mar. Pollut. Bull.* 73, 319–326. <https://doi.org/10.1016/j.marpolbul.2013.05.020>.

- Camilli, R., Iorio, D.D., Bowen, A., Reddy, C.M., Techet, A.H., Yoerger, D.R., Whitcomb, L.L., Seewald, J.S., Sylva, S.P., Fenwick, J., 2012. Acoustic measurement of the Deepwater Horizon Macondo well flow rate. *Proc. Natl. Acad. Sci.* 109, 20235–20239. <https://doi.org/10.1073/pnas.1100385108>.
- Carnahan, N.F., Salager, J.-L., Antón, R., Dávila, A., 1999. Properties of resins extracted from Boscan crude oil and their effect on the stability of asphaltenes in Boscan and Hamaca crude oils. *Energy Fuel* 13, 309–314. <https://doi.org/10.1021/ef980218v>.
- Chen, D.H., Dinivahi, M.V., Jeng, C.Y., 1993. New acentric factor correlation based on the Antoine equation. *Ind. Eng. Chem. Res.* 32, 241–244. <https://doi.org/10.1021/ie00013a034>.
- Clift, R., Grace, J.R., Weber, M.E., 1978. *Bubbles, Drops, and Particles*. Academic Press, New York.
- Danesh, A., 1998. *PVT and Phase Behaviour of Petroleum Reservoir Fluids*, Elsevier. ed. Developments in Petroleum Science, Amsterdam.
- de Hemptinne, J.-C., Delepine, H., Jose, C., Jose, J., 1998. Aqueous solubility of hydrocarbon mixtures. *Rev. Inst. Français Pet.* 53, 409–419.
- Dhima, A., de Hemptinne, J.-C., Morachini, G., 1998. Solubility of light hydrocarbons and their mixtures in pure water under high pressure. *Fluid Phase Equilib.* 145, 129–150. [https://doi.org/10.1016/S0378-3812\(97\)00211-2](https://doi.org/10.1016/S0378-3812(97)00211-2).
- Dhima, A., de Hemptinne, J.-C., Jose, J., 1999. Solubility of hydrocarbons and CO₂ mixtures in water under high pressure. *Ind. Eng. Chem. Res.* 38, 3144–3161. <https://doi.org/10.1021/ie980768g>.
- Dissanayake, A.L., Socolofsky, S.A., 2015. Numerical models to simulate oil and gas blowout plumes and associated chemical and physical processes of hydrocarbons. In: *E-Proceedings of the 36th IAHR World Congress*. The Hague.
- Dissanayake, A.L., Burd, A.B., Daly, K.L., Francis, S., Passow, U., 2018a. Numerical modeling of the interactions of oil, marine snow, and riverine sediments in the ocean. *J. Geophys. Res. Oceans*. <https://doi.org/10.1029/2018JC013790>.
- Dissanayake, A.L., Gros, J., Socolofsky, S.A., 2018b. Integral models for bubble, droplet, and multiphase plume dynamics in stratification and cross flow. *Environ. Fluid Mech.* 1–36.
- Fan, L.-S., Yang, G.Q., Lee, D.J., Tsuchiya, K., Luo, X., 1999. Some aspects of high-pressure phenomena of bubbles in liquids and liquid–solid suspensions. *Chem. Eng. Sci.* 54, 4681–4709. [https://doi.org/10.1016/S0009-2509\(99\)00348-6](https://doi.org/10.1016/S0009-2509(99)00348-6).
- Fan, T., Wang, J., Buckley, J.S., 2002. Evaluating crude oils by SARA analysis. In: *Presented at the SPE/DOE Improved Oil Recovery Symposium*. Society of Petroleum Engineers. <https://doi.org/10.2118/75228-MS>.
- Fingas, M., 2017. Chapter 15 - Deepwater Horizon well blowout mass balance. In: *Oil Spill Science and Technology*, Second edition. Gulf Professional Publishing, Boston, pp. 805–849.
- Firoozabadi, A., Ramey, H.J., 1988. Surface tension of water-hydrocarbon systems at reservoir conditions. *J. Can. Pet. Technol.* 27, 41–48. <https://doi.org/10.2118/88-03-03>.
- French McCay, D., Jayko, K., Li, Z., Horn, M., Kim, Y., Isaji, T., Crowley, D., Spaulding, M., Decker, L., Turner, C., Zamorski, S., Fontenault, J., Shmookler, R., Rowe, J., 2015a. *Technical Reports for Deepwater Horizon Water Column Injury Assessment WC.TR.14: Modeling Oil Fate and Exposure Concentrations in the Deepwater Plume and Rising Oil Resulting From the Deepwater Horizon Oil Spill*. RPS ASA, South Kingstown.
- French McCay, D., Rowe, J., Balouskus, R., Morandi, A., Conor McManus, M., 2015b. *Technical Reports for Deepwater Horizon Water Column Injury Assessment WC.TR.28: Injury Quantification for Planktonic Fish and Invertebrates in Estuarine, Shelf and Offshore Waters*. RPS ASA, South Kingstown, RI.
- Government of Canada, E.C., 2017. *ETC Spills Technology Databases, Oil Properties Database*. WWW Document. <http://www.etc-cte.ec.gc.ca/databases/oilproperties/>, Accessed date: 24 May 2017.
- Gros, J., 2016. *Investigating the Fate of Petroleum Fluids Released in the Marine Environment With Comprehensive Two-Dimensional Gas Chromatography and Transport Models* (Ph.D. Dissertation). École Polytechnique Fédérale de Lausanne, Lausanne.
- Gros, J., Nabi, D., Würz, B., Wick, L.Y., Brussaard, C.P.D., Huisman, J., van der Meer, J.R., Reddy, C.M., Arey, J.S., 2014. First day of an oil spill on the open sea: early mass transfers of hydrocarbons to air and water. *Environ. Sci. Technol.* 48, 9400–9411. <https://doi.org/10.1021/es502437e>.
- Gros, J., Reddy, C.M., Nelson, R.K., Socolofsky, S.A., Arey, J.S., 2016. Simulating gas–liquid–water partitioning and fluid properties of petroleum under pressure: implications for deep-sea blowouts. *Environ. Sci. Technol.* 50, 7397–7408. <https://doi.org/10.1021/acs.est.5b04617>.
- Gros, J., Socolofsky, S.A., Dissanayake, A.L., Jun, I., Zhao, L., Boufadel, M.C., Reddy, C.M., Arey, J.S., 2017. Petroleum dynamics in the sea and influence of subsurface dispersant injection during *Deepwater Horizon*. *Proc. Natl. Acad. Sci.* 201612518. <https://doi.org/10.1073/pnas.1612518114>.
- Harrison, W., Winnik, M.A., Kwong, P.T.Y., MacKay, D., 1975. Disappearance of aromatic and aliphatic components from small sea-surface slicks. *Environ. Sci. Technol.* 9, 231–234.
- Hayduk, W., Laudie, H., 1974. Prediction of diffusion coefficients for nonelectrolytes in dilute aqueous solutions. *AIChE J.* 20, 611–615. <https://doi.org/10.1002/aic.690200329>.
- Hine, J., Mookerjee, P.K., 1975. Structural effects on rates and equilibria. XIX. Intrinsic hydrophilic character of organic compounds. Correlations in terms of structural contributions. *J. Organomet. Chem.* 40, 292–298. <https://doi.org/10.1021/jo00891a006>.
- Johansen, Ø., 2003. Development and verification of deep-water blowout models. *Mar. Pollut. Bull.* 47, 360–368. [https://doi.org/10.1016/S0025-326X\(03\)00202-9](https://doi.org/10.1016/S0025-326X(03)00202-9).
- Johansen, Ø., Brandvik, P.J., Farooq, U., 2013. Droplet breakup in subsurface oil releases – part 2: predictions of droplet size distributions with and without injection of chemical dispersants. *Mar. Pollut. Bull.* 73, 327–335. <https://doi.org/10.1016/j.marpolbul.2013.04.012>.
- Kalantari Meybodi, M., Daryasafar, A., Karimi, M., 2016. Determination of hydrocarbon-water interfacial tension using a new empirical correlation. *Fluid Phase Equilib.* 415, 42–50. <https://doi.org/10.1016/j.fluid.2016.01.037>.
- Kim, H., Burgess, D.J., 2001. Prediction of interfacial tension between oil mixtures and water. *J. Colloid Interface Sci.* 241, 509–513. <https://doi.org/10.1006/jcis.2001.7655>.
- King, M.B., 1969. *Phase Equilibrium in Mixtures*, International Series of Monographs in Chemical Engineering. Pergamon Press, Oxford.
- Krichevsky, I.R., Kasarnovsky, J.S., 1935. Thermodynamical calculations of solubilities of nitrogen and hydrogen in water at high pressures. *J. Am. Chem. Soc.* 57, 2168–2171. <https://doi.org/10.1021/ja01314a036>.
- Lee, J.H.W., Cheung, V., 1990. Generalized Lagrangian model for buoyant jets in current. *J. Environ. Eng.* 116, 1085–1106. [https://doi.org/10.1061/\(ASCE\)0733-9372\(1990\)116:6\(1085\)](https://doi.org/10.1061/(ASCE)0733-9372(1990)116:6(1085)).
- Lee, B.I., Kesler, M.G., 1975. A generalized thermodynamic correlation based on three-parameter corresponding states. *AIChE J.* 21, 510–527. <https://doi.org/10.1002/aic.690210313>.
- Lehr, W.J., Overstreet, R., Jones, R., Watabayashi, G., 1992. ADIOS-automated data inquiry for oil spills. In: *Proceedings of the 15th Arctic Marine Oilspill Program, Technical Seminar*. Environment Canada, Ottawa, Ontario, pp. 31–45.
- Lehr, W., Wesley, D., Simecek-Beatty, D., Jones, R., Kachook, G., Lankford, J., 2000. Algorithm and interface modifications of the NOAA oil spill behavior model. In: *Proceedings of the 23rd Arctic and Marine Oil Spill Program (AMOP) Technical Seminar*. Environment Canada, Vancouver, BC, pp. 525–539.
- Lehr, W., Jones, R., Evans, M., Simecek-Beatty, D., Overstreet, R., 2002. Revisions of the ADIOS oil spill model. *Environ. Model. Softw.* 17, 189–197. [https://doi.org/10.1016/S1364-8152\(01\)00064-0](https://doi.org/10.1016/S1364-8152(01)00064-0).
- Li, P., Niu, H., Li, S., Fernandes, R., Neves, R., 2017. A comprehensive system for simulating oil spill trajectory and behaviour in subsurface and surface water environments. *Int. Oil Spill Conf. Proc.* 2017, 1251–1266. <https://doi.org/10.7901/2169-3358-2017.1.1251>.
- Li, Z., Spaulding, M., French McCay, D., Crowley, D., Payne, J.R., 2017. Development of a unified oil droplet size distribution model with application to surface breaking waves and subsea blowout releases considering dispersant effects. *Mar. Pollut. Bull.* 114, 247–257. <https://doi.org/10.1016/j.marpolbul.2016.09.008>.
- Lin, H., Duan, Y.-Y., 2005. Empirical correction to the Peng–Robinson equation of state for the saturated region. *Fluid Phase Equilib.* 233, 194–203. <https://doi.org/10.1016/j.fluid.2005.05.008>.
- Lyckman, E.W., Eckert, C.A., Prausnitz, J.M., 1965. Generalized reference fugacities for phase equilibrium thermodynamics. *Chem. Eng. Sci.* 20, 685–691. [https://doi.org/10.1016/0009-2509\(65\)80005-7](https://doi.org/10.1016/0009-2509(65)80005-7).
- McCain Jr., W.D., 1990. *The Properties of Petroleum Fluids*. PennWell Publishing Company, Tulsa.
- McNutt, M.K., Camilli, R., Crone, T.J., Guthrie, G.D., Hsieh, P.A., Ryerson, T.B., Savas, O., Shaffer, F., 2012. Review of flow rate estimates of the *Deepwater Horizon* oil spill. *Proc. Natl. Acad. Sci.* 109, 20260–20267. <https://doi.org/10.1073/pnas.1112139108>.
- Millero, F.J., 1986. The thermodynamics and kinetics of the hydrogen sulfide system in natural waters. *Mar. Chem.* 18, 121–147. [https://doi.org/10.1016/0304-4203\(86\)90003-4](https://doi.org/10.1016/0304-4203(86)90003-4).
- Najafi-Marghaleki, A., Tatar, A., Barati-Harooni, A., Mohebbi, A., Kalantari-Meybodi, M., Mohammadi, A.H., 2016. On the prediction of interfacial tension (IFT) for water-hydrocarbon gas system. *J. Mol. Liq.* 224, 976–990. <https://doi.org/10.1016/j.molliq.2016.10.083>.
- Nissanka, I.D., Yapa, P.D., 2016. Calculation of oil droplet size distribution in an under-water oil well blowout. *J. Hydraul. Res.* 54, 307–320. <https://doi.org/10.1080/00221686.2016.1144656>.
- Oil in the Sea III: Inputs, Fates, and Effects. The National Academies Press, Washington, DC.
- Papavasileiou, K.D., Moulton, O.A., Economou, I.G., 2017. Predictions of water/oil interfacial tension at elevated temperatures and pressures: a molecular dynamics simulation study with biomolecular force fields. *Fluid Phase Equilib.* <https://doi.org/10.1016/j.fluid.2017.05.004>.
- Passow, U., Ziervogel, K., Asper, V., Diercks, A., 2012. Marine snow formation in the aftermath of the *Deepwater Horizon* oil spill in the Gulf of Mexico. *Environ. Res. Lett.* 7, 35301. <https://doi.org/10.1088/1748-9326/7/3/035301>.
- Pedersen, K.S., Thomassen, P., Fredenslund, A., 1988. On the dangers of “tuning” equation of state parameters. *Chem. Eng. Sci.* 43 (2), 269–278 (<https://doi.org/NA>).
- Pedersen, K.S., Christensen, P.L., Shaikh, G.A., 2014. *Phase Behavior of Petroleum Reservoir Fluids*, 2nd ed. CRC Press, Boca Raton, Florida.
- Peng, D.-Y., Robinson, D.B., 1976. A new two-constant equation of state. *Ind. Eng. Chem. Fundam.* 15, 59–64. <https://doi.org/10.1021/i160057a011>.
- Pilcher, K.A., Winterbottom, J.M., 1988. The stability of crude oil residues and factors affecting their decomposition during mild thermal treatment. *Chem. Eng. Technol.* 11, 89–94. <https://doi.org/10.1002/ceat.270110113>.
- Poling, B.E., Prausnitz, J.M., O’Connell, J.P., 2001. *The Properties of Gases and Liquids*, 5th ed. McGraw-Hill.
- Radović, J.R., Domínguez, C., Laffont, K., Díez, S., Readman, J.W., Albaigés, J., Bayona, J.M., 2012. Compositional properties characterizing commonly transported oils and controlling their fate in the marine environment. *J. Environ. Monit.* 14, 3220–3229. <https://doi.org/10.1039/C2EM30385J>.
- Reddy, C.M., Arey, J.S., Seewald, J.S., Sylva, S.P., Lemkau, K.L., Nelson, R.K., Carmichael, C.A., McIntyre, C.P., Fenwick, J., Ventura, G.T., Mooy, B.A.S.V., Camilli, R., 2012. Composition and fate of gas and oil released to the water column during the

- Deepwater Horizon oil spill. Proc. Natl. Acad. Sci. 109, 20229–20234. <https://doi.org/10.1073/pnas.1101242108>.
- Reed, M., Johansen, Ø., Brandvik, P.J., Daling, P., Lewis, A., Fiocco, R., MacKay, D., Prentki, R., 1999. Oil spill modeling towards the close of the 20th century: overview of the state of the art. Spill Sci. Technol. Bull. 5, 3–16. [https://doi.org/10.1016/S1353-2561\(98\)00029-2](https://doi.org/10.1016/S1353-2561(98)00029-2).
- Reed, M., Daling, P.S., Brakstad, O.G., Singsaas, I., Faksness, L.-G., Hetland, B., Ekrol, N., 2000. OSCAR2000: A multi-component 3-dimensional oil spill contingency and response model. In: Proceedings of the 23rd Arctic and Marine Oil Spill Program (AMOP) Technical Seminar. Vancouver, BC, Environment Canada, pp. 663–680.
- Riazi, M.R., 2005. Characterization and Properties of Petroleum Fractions. American Society for Testing and Materials.
- Robinson, D.B., Peng, D.-Y., 1978. The Characterization of the Heptanes and Heavier Fractions for the GPA Peng-Robinson Programs (no. Research Report 28). Gas Processors Association, Tulsa.
- Ryerson, T.B., Camilli, R., Kessler, J.D., Kujawinski, E.B., Reddy, C.M., Valentine, D.L., Atlas, E., Blake, D.R., de Gouw, J., Meinardi, S., Parrish, D.D., Peischl, J., Seewald, J.S., Warneke, C., 2012. Chemical data quantify Deepwater Horizon hydrocarbon flow rate and environmental distribution. Proc. Natl. Acad. Sci. 109, 20246–20253. <https://doi.org/10.1073/pnas.1110564109>.
- Schwarzenbach, R.P., Gschwend, P.M., Imboden, D.M., 2003. Environmental Organic Chemistry, 2nd ed. John Wiley & Sons, Inc., Hoboken.
- Shakir, S., de Hemptinne, J.-C., 2007. The effect of diffusion on the modeling of the water-washing phenomenon. J. Pet. Sci. Eng. 58, 403–412. <https://doi.org/10.1016/j.petrol.2006.04.022>.
- Socolofsky, S.A., 2017. TAMOC. (College Station).
- Socolofsky, S.A., Bhaumik, T., Seol, D.-G., 2008. Double-plume integral models for near-field mixing in multiphase plumes. J. Hydraul. Eng. 134, 772–783. [https://doi.org/10.1061/\(ASCE\)0733-9429\(2008\)134:6\(772\)](https://doi.org/10.1061/(ASCE)0733-9429(2008)134:6(772)).
- Socolofsky, S.A., Adams, E.E., Sherwood, C.R., 2011. Formation dynamics of subsurface hydrocarbon intrusions following the Deepwater Horizon blowout. Geophys. Res. Lett. 38, L09602. <https://doi.org/10.1029/2011GL047174>.
- Socolofsky, S.A., Adams, E.E., Boufadel, M.C., Aman, Z.M., Johansen, Ø., Konkel, W.J., Lindo, D., Madsen, M.N., North, E.W., Paris, C.B., Rasmussen, D., Reed, M., Rønningen, P., Sim, L.H., Uhrenholdt, T., Anderson, K.G., Cooper, C., Nedwed, T.J., 2015a. Intercomparison of oil spill prediction models for accidental blowout scenarios with and without subsea chemical dispersant injection. Mar. Pollut. Bull. 96, 110–126. <https://doi.org/10.1016/j.marpolbul.2015.05.039>.
- Socolofsky, S.A., Dissanayake, A.L., Jun, I., Gros, J., Arey, J.S., Reddy, C.M., 2015b. Texas A&M Oilspill Calculator (TAMOC) modeling suite for subsea spills. In: Proceedings of the Thirty-Eighth AMOP Technical Seminar. Environment Canada, Ottawa, pp. 153–168.
- Spaulding, M.L., 2017. State of the art review and future directions in oil spill modeling. Mar. Pollut. Bull. 115, 7–19. <https://doi.org/10.1016/j.marpolbul.2017.01.001>.
- Spaulding, M.L., Howlett, E., Anderson, E., Jayko, K., 1992. OILMAP: A global approach to spill modeling. In: Presented at the 15th Arctic and Marine Oil Spill Program, Technical Seminar, Edmonton, Alberta, Canada, pp. 15–21.
- Spaulding, M., Mendelsohn, D., Crowley, D., Li, Z., Bird, A., 2015. Technical Reports for Deepwater Horizon Water Column Injury Assessment WC_TR.13: Application of OILMAP DEEP to the Deepwater Horizon blowout. RPS ASA, South Kingstown.
- Stout, S.A., Wang, Z., 2007. Chemical fingerprinting of spilled or discharged petroleum — Methods and factors affecting petroleum fingerprints in the environment. In: Wang, Z., Stout, S.A. (Eds.), Oil Spill Environmental Forensics. Academic Press, Burlington, pp. 1–53.
- Twu, C.H., 1984. An internally consistent correlation for predicting the critical properties and molecular weights of petroleum and coal-tar liquids. Fluid Phase Equilib. 16, 137–150. [https://doi.org/10.1016/0378-3812\(84\)85027-X](https://doi.org/10.1016/0378-3812(84)85027-X).
- Wang, B., Socolofsky, S.A., Lai, C.C.K., Adams, E.E., Boufadel, M.C., 2018. Behavior and dynamics of bubble breakup in gas pipeline leaks and accidental subsea oil well blowouts. Mar. Pollut. Bull. 131, 72–86.
- White, H.K., Hsing, P.-Y., Cho, W., Shank, T.M., Cordes, E.E., Quattrini, A.M., Nelson, R.K., Camilli, R., Demopoulos, A.W.J., German, C.R., Brooks, J.M., Roberts, H.H., Shedd, W., Reddy, C.M., Fisher, C.R., 2012. Impact of the Deepwater Horizon oil spill on a deep-water coral community in the Gulf of Mexico. Proc. Natl. Acad. Sci. 109, 20303–20308. <https://doi.org/10.1073/pnas.1118029109>.
- Wilhelm, E., Battino, R., Wilcock, R.J., 1977. Low-pressure solubility of gases in liquid water. Chem. Rev. 77, 219–262. <https://doi.org/10.1021/cr60306a003>.
- Xie, W.-H., Shiu, W.-Y., MacKay, D., 1997. A review of the effect of salts on the solubility of organic compounds in seawater. Mar. Environ. Res. 44, 429–444. [https://doi.org/10.1016/S0141-1136\(97\)00017-2](https://doi.org/10.1016/S0141-1136(97)00017-2).
- Young, A.F., Pessoa, F.L.P., Ahn, V.R.R., 2017. Comparison of volume translation and co-volume functions applied in the Peng-Robinson EoS for volumetric corrections. Fluid Phase Equilib. 435, 73–87. <https://doi.org/10.1016/j.fluid.2016.12.016>.
- Zelenke, B., O'Connor, C., Barker, C., Beegle-Krause, C.J., 2012a. General NOAA Operational Modeling Environment (GNOME) Technical Documentation: Data formats, NOAA Technical Memorandum NOS OR&R 41. Emergency Response Division, Seattle, WA.
- Zelenke, B., O'Connor, C., Barker, C., Beegle-Krause, C.J., Eclipse, L., 2012b. General NOAA Operational Modeling Environment (GNOME) Technical Documentation, NOAA Technical Memorandum NOS OR &R 40. Emergency Response Division, Seattle, WA.
- Zhao, L., Boufadel, M.C., Socolofsky, S.A., Adams, E., King, T., Lee, K., 2014. Evolution of droplets in subsea oil and gas blowouts: development and validation of the numerical model VDRO-J. Mar. Pollut. Bull. 83, 58–69. <https://doi.org/10.1016/j.marpolbul.2014.04.020>.
- Zhao, L., Boufadel, M.C., King, T., Robinson, B., Gao, F., Socolofsky, S.A., Lee, K., 2017. Droplet and bubble formation of combined oil and gas releases in subsea blowouts. Mar. Pollut. Bull. 120, 203–216. <https://doi.org/10.1016/j.marpolbul.2017.05.010>.
- Zheng, L., Yapa, P.D., Chen, F., 2003. A model for simulating Deepwater oil and gas blowouts - part I: theory and model formulation. J. Hydraul. Res. 41, 339–351. <https://doi.org/10.1080/00221680309499980>.
- Zick, A.A., 2013a. Equation-of-State Fluid Characterization and Analysis of the Macondo Reservoir Fluids (Expert Report Prepared on Behalf of the United States No. TREX-011490R).
- Zick, A.A., 2013b. Expert Rebuttal Report (Prepared on Behalf of the United States No. TREX-011491R).